

# Stretch-activated Current through Single Ion Channels in the Abdominal Stretch Receptor Organ of the Crayfish

CHRISTIAN ERXLEBEN

From the Department of Biology, University of Konstanz, D7750 Konstanz, Federal Republic of Germany

**ABSTRACT** Single stretch-activated ion channels were studied on the soma and primary dendrites of stretch receptor neurons of the crayfish *Orconectes limosus*. When the membrane of the patch was deformed by applying suction to the pipette, a marked nonlinear increase in single-channel activity could be observed in two types of channels. These were indistinguishable on the basis of their single-channel conductances but differed in their voltage range of activation. One type showed strong inward rectification (RSA channel) and the second type was largely voltage independent (SA channel). A linear relationship was found between negative pressure and the natural logarithm of the channels' open probability. For an  $e$ -fold change in pressure, the average sensitivity was  $8.7 \pm 0.4$  (SD,  $n = 5$ ) mmHg for the RSA channel and  $5.6 \pm 2.2$  ( $n = 5$ ) mmHg for the SA channel. Both channels were found to be permeable to mono- and divalent cations. Current-voltage relationships were linear with slope conductances for the SA channel of:  $71 \pm 11$  (SD,  $n = 3$ ) pS for  $K^+$ ,  $50 \pm 7.4$  ( $n = 5$ ) pS for  $Na^+$ , and 23 pS for  $Ca^{++}$ . Similar values were found for the RSA channel. The data suggest that the SA channel is responsible for the mechanotransduction process in the stretch receptor neuron.

## INTRODUCTION

Primary transduction processes of receptor neurons are generally believed to be linked to the opening of ionic channels. Little is known about the channels involved in mechanoreception since the actual transduction site, i.e., the kinocilium of a hair cell or the Pacinian corpuscle, is not directly accessible for single-channel patch-clamp recordings.

As a prototype of a mechano-sensitive ion channel a stretch-activated channel from tissue-cultured embryonic chick muscle cells has been proposed (Guharay and Sachs, 1984, 1985). Similar types of stretch-activated channels were found in muscle cells and oocytes of *Xenopus* (Brehm et al., 1984; Methfessel et al., 1986) and in heart ventricle cells of *Lymnea stagnalis* (Sigurdson et al., 1987). The physiological significance of mechano-sensitive channels in these preparations, however, remains unclear.

Address reprint requests to Dr. Christian Erxleben, Department of Biology, University of Konstanz, Postfach 5560, D7750 Konstanz 1, West Germany.

Size and accessibility of the crustacean stretch receptor preparation (Alexandrowicz, 1951) make it particularly suited to test if such stretch-activated channels also exist in a cell with known mechanoreceptive function.

A preliminary report of this work was published in abstract form (Erxleben and Florey, 1988).

#### MATERIALS AND METHODS

##### *Preparation*

Crayfish *Orconectes limosus* were obtained from a commercial supplier (Fischerei Liptow, Berlin, FRG) and kept at 13–17°C in running fresh water. The receptor organs, consisting of a fast and slowly adapting receptor cell and the corresponding muscle fibers, were isolated from the second to fifth abdominal segments of the animals. The preparation was pinned at the approximate in situ length in a Sylgard 184-lined (Dow Corning Corp., Midland, MI) experimental chamber and submerged in saline. Experiments were performed at ambient temperature (20–24°C).

To obtain gigaohm seals the preparation was treated locally with protease (10 mg/ml, type XIV; Sigma Chemical Corp., St. Louis, MO). A polished pipette with an opening of ~25  $\mu\text{m}$  was filled with saline containing protease and was positioned onto the receptor cell. An exposure of 5–10 min, depending on the extent of connective tissue, was sufficient to make the surface accessible for patch-clamp recordings.

##### *Electrophysiological Techniques and Data Analysis*

Single-channel currents were recorded with an EPC-7 (List Electronic, Darmstadt, FRG) patch-clamp amplifier in the cell-attached or excised inside-out configuration. Recording techniques were those of Hamill et al. (1981) and the patch electrodes (diameter, ~2  $\mu\text{m}$ ) were coated with polystyrene (Q-Dope, GC Electronics, Rockford, IL) or Sylgard 184 (Dow Corning). Membrane tension was controlled via a 100- $\mu\text{l}$  syringe connected to the patch electrode holder and a calibrated pressure transducer (Hugo Sachs Elektronik, March-Hugstetten, FRG). Data were either stored on magnetic tape with a FM recorder (Racall, Southampton, UK) for later analysis or directly digitized by a 12-bit A/D converter (1401 labinterface; CED Cambridge, UK) in connection with a PC (Tandon PCA 40, Chatsworth, CA). Data were filtered (six-pole Bessel filter) at 3 kHz for the analysis, and at 1 kHz for the preparation of figures. The sampling rate was five times the filter frequency. Data acquisition and analysis were performed by a commercially available patch-clamp program (CED). SYSTAT (Systat Inc., Evanston, IL) was used for statistical analyses and curvefits. Single-channel current amplitudes and dwell times were determined by a multilevel analysis routine using the 50% amplitude level for detection of channel openings. Open probabilities ( $P_o$ ) were obtained by summation of open times. Downward deflection of the current traces correspond to inward currents.

##### *Solutions*

The compositions of all salines are given in Table I. Normal saline was used as bath solution and on the cytoplasmic side of excised inside-out patches.

#### RESULTS

##### *Determination of the Patch Recording Site*

The crustacean abdominal stretch receptor neuron is surrounded not only by connective tissue but also by glial cells (Nadol and De Lorenzo, 1973; Fischer et al.,

TABLE 1  
*Composition of Salines*

	NaCl	KCl	CaCl <sub>2</sub>	MgCl <sub>2</sub>	HEPES	Tris	EGTA
Normal	195	5.4	13.5	2.6	0	10	0
High K <sup>+</sup>	0	160	13.5	2.6	10	0	0
High K <sup>+</sup> , low Ca <sup>++</sup>	0	160	1	1	10	0	1.5
High Ca <sup>++</sup>	0	0	110	0	10	0	0
High Na <sup>+</sup>	175	5.4	13.5	2.6	0	10	0

Concentrations are given in millimolar. The pH was adjusted to 7.4 with NaOH or KOH where appropriate.

1975; Tao-Cheng et al., 1981). Thus it was crucial to determine whether patches were from such glial cells or from the receptor neuron itself. Two different types of patches were obtained. 90–95% of all patches typically showed a voltage-independent K<sup>+</sup> channel. In the whole-cell clamp mode, voltage response to current pulses showed a fast (steeper than exponential or error function) rising phase that is typical for sheet-like cells (Woodbury and Crill, 1961). Together with electrical inexcitability this was taken as evidence for recordings on glial cells.

The remaining patches were on the neuron. In the cell-attached configuration they were identified on the basis of capacitive components of action potentials of spontaneously active neurons. In the whole-cell current-clamp mode obtained by rupturing the patch by a strong suction pulse on the pipette, the corresponding intracellular action potentials could be recorded (Fig. 1).

#### *Increase in Channel Activity with Suction*

During seal formation it became apparent that patches on the neuron contained channels that responded to suction on the pipette (Fig. 2). Two types of stretch-activated channels were observed. They were indistinguishable on the basis of their

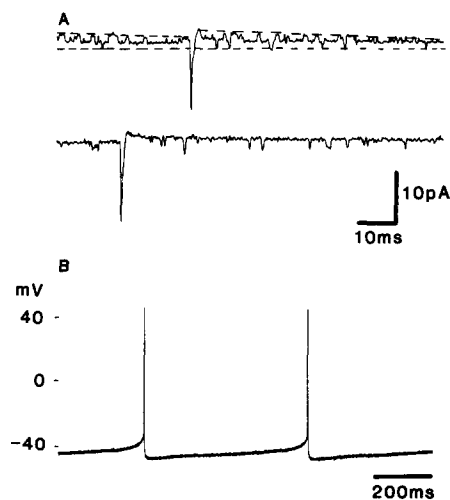


FIGURE 1. Action potentials from a crayfish stretch receptor neuron. (A) Capacitive components of spontaneous action potentials in a cell-attached patch with a high K<sup>+</sup>, low Ca<sup>++</sup> solution in the pipette, and the holding potential kept at the cell's resting potential. Dotted lines in the upper trace mark the closed and open levels of channels. Note the decrease and increase in single-channel amplitude just before and after the action potentials, respectively. (B) Whole-cell current-clamp recording after rupturing the patch by a strong suction pulse. A different neuron than in A, high K<sup>+</sup>, low Ca<sup>++</sup> solution in the pipette.

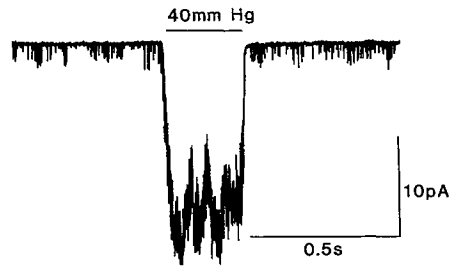


FIGURE 2. Activation of an inward current by negative pressure. Cell-attached patch with high  $K^+$  solution in the pipette, patch potential at cell membrane potential. During the time indicated, suction was applied to the pipette.

ion selectivity or single-channel conductance but differed in their sensitivity to membrane deformation and voltage range of activation.

The first type of channel was virtually inactive in the absence of suction to the pipette and showed at most a few bursts per minute. The probability of the channel being open increased with hyperpolarization (Fig. 3). This channel is subsequently referred to as the inwardly rectifying stretch-activated (RSA) channel. The second type of channel was only weakly voltage dependent (Fig. 3) and its average basal activity in the absence of suction was about an order of magnitude higher than that of the RSA channel (mean  $P_o$  RSA:  $9 \times 10^{-4}$ , mean  $P_o$  SA:  $1.3 \times 10^{-2}$ ). This channel will be referred to simply as the stretch-activated (SA) channel. A total of 24 patches from the slow- and fast-adapting neuron could be obtained. In general, patches from the region of the primary dendrites had channels of the SA type with a large number of channels in the patch (i.e., Fig. 2). Those on the cell body or axon hillock

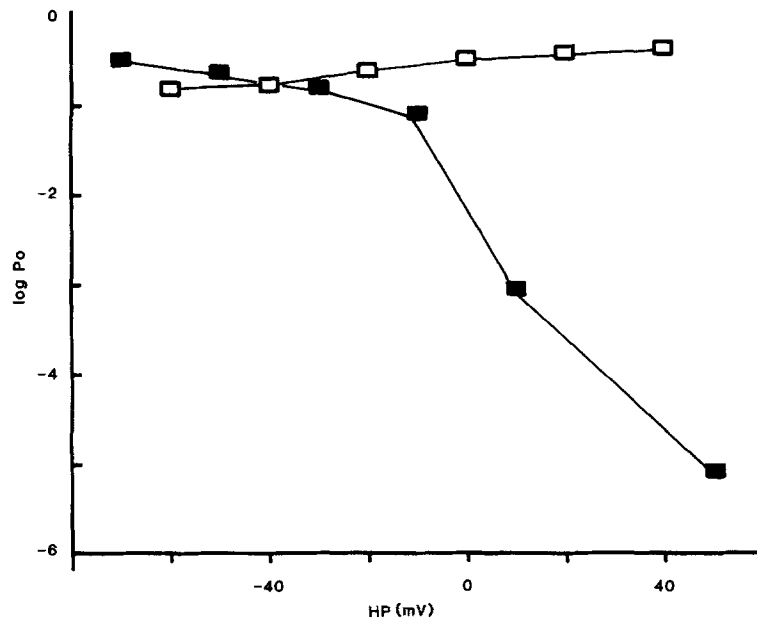


FIGURE 3. Voltage dependence of the SA and RSA channels open probabilities. ( $\square$ ), SA channel at 10 mmHg suction. ( $\blacksquare$ ), RSA channel at 28 mmHg suction. Cell-attached patches, high  $Na^+$  solution in the pipette. Potentials are relative to the cells' resting potentials.

mainly had RSA channels with fewer channels in the patch. Although experiments were not designed for excised patches (i.e., patches were only excised after measurements had been carried out in the cell-attached configuration) it was obvious that sensitivity to suction was not confined to cell-attached patches. In the case of the RSA channel, activity showed "run down," typically down to 25% within 5 min after excision of the patch. In excised patches with SA channels, however, activity increased after excision and subsequent application of either pressure or suction resulted in a transient decrease of activity.

Other types of channels, such as a delayed-rectifying  $K^+$  channel which was sometimes present in the same patch as the stretch-activated channels, did not respond to suction. Fig. 4 shows sequences from a cell-attached patch with two RSA and several voltage-dependent  $K^+$  channels. Both types of channels could be studied in isolation: at membrane resting potential ( $-65$  to  $-70$  mV) or more negative potentials,

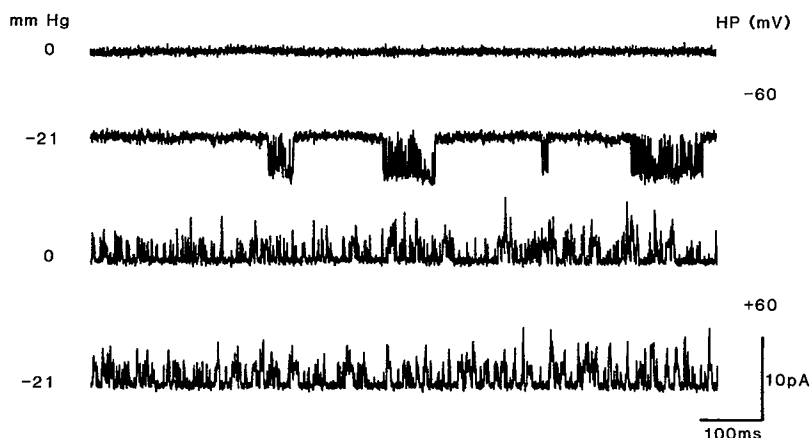


FIGURE 4. Stretch-activated (RSA) and stretch-insensitive channels in the same patch. Cell-attached patch with high  $Na^+$  solution in the pipette. Stretch-activated channels recorded at a patch potential  $-60$  mV from cell membrane potential and voltage-dependent  $K^+$  channels at  $+60$  mV, respectively. The upper trace of each set shows channel activity at  $0$  mmHg and the lower trace at  $-21$  mmHg.

only the stretch-activated channel was active. During depolarization by  $60$  mV, only openings of the  $K^+$  channel were apparent. The open probability of the RSA channel in this patch increased some 55-fold from  $P_o = 0.0013$  to  $P_o = 0.0718$  while changing from  $0$  mmHg suction to  $-21$  mmHg. In contrast, the open probability of the voltage-dependent  $K^+$  channel did not change significantly ( $P_o = 0.28$  at  $0$  mmHg,  $P_o = 0.26$  at  $-21$  mmHg). Furthermore, patches that originated from the glial cells also never showed pressure-sensitive channels.

#### *Relationship between Membrane Tension and Open Probability*

Whereas the general effect of an increase in negative pressure is best demonstrated in a recording with many channels (Fig. 2), patches with few channels, and preferably just one, are suited for a more quantitative description of the tension vs. open

probability relationship. For this purpose activity of RSA and SA channels was recorded over periods of several minutes at different levels of constant suction (Fig. 5). With increasing suction, channel activity increased in a nonlinear fashion. At constant suction, mean channel activity remained constant. Suction in excess of some 50 mmHg resulted in a shift of baseline current, increased current noise, and, finally, breakdown of the seal.

To determine the absolute open probabilities, the number of channels in a given patch had to be known. It was estimated from recordings at the highest activity as the maximum number of simultaneous openings observed. In the case of the RSA channel,  $P_o$  never reached saturation within the range of suction that was tolerated by the membrane. Consequently, the estimated number of channels in a patch can only be regarded as approximate. The relationship between suction and open probability for a patch with an RSA channel is shown in Fig. 6. While the absolute open probabilities varied between patches, the pressure sensitivities were remarkably sim-

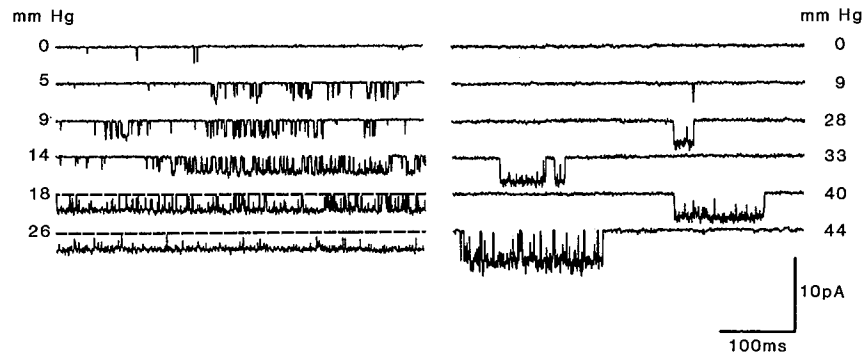


FIGURE 5. Unitary currents through SA (*left*) and RSA (*right*) stretch-activated channels. Data from cell-attached patches with high  $\text{Na}^+$  solution in the pipette. Holding potentials were at the cell's resting potential (SA) and  $-50$  mV from the cell's resting potential (RSA), respectively. Nonconsecutive traces during constant suction levels as indicated.

ilar. Sensitivities were calculated from a maximum-likelihood fit to the data with Boltzmann curves of the form:

$$P_o = 1/[1 + k * \exp (s * p)] \quad (1)$$

or

$$P_o = 1/[1 + k * \exp (s * p^2)] \quad (2)$$

with  $k$  being a pressure insensitive term,  $s$  the sensitivity, and  $p$  denoting the applied negative pressure in mmHg for Eq. 1 and the square of pressure  $p^2$  for Eq. 2. The average sensitivity for the RSA channels was  $0.115 \pm 0.05 \text{ mmHg}^{-1}$  (SD,  $n = 5$ ) for the linear, and  $0.195 \pm 0.07 \text{ cmHg}^{-2}$  for the (pressure)<sup>2</sup> model.

In contrast to the RSA channel, the open probability of the SA channel saturated within the range of applicable suction. Fig. 6 shows an example of the suction vs.  $P_o$  relationship for an SA channel. Fitted with Eqs. 1 and 2 the average sensitivity was

$0.178 \pm 0.12 \text{ mmHg}^{-1}$  ( $n = 5$ ) for the linear, and  $0.711 \pm 0.73 \text{ cmHg}^{-2}$  for the (pressure)<sup>2</sup> model. Both models are evaluated in the Discussion.

#### *Current-Voltage Relationships and Single-Channel Conductances*

Voltage-clamp data of the stretch-induced receptor current in the crayfish stretch receptor (Edwards et al., 1981) suggest that the mechanotransduction channel should not only be permeable to  $\text{Na}^+$ , the main charge carrier under physiological conditions, but also to  $\text{K}^+$  and divalent cations such as  $\text{Ca}^{++}$ . Therefore the ion selectivity for the putative transduction channels was determined in cell-attached patches in which either  $\text{K}^+$  or  $\text{Ca}^{++}$  replaced the  $\text{Na}^+$  in the pipette solution. Both of these cations were also able to carry current through the SA channel. Current-voltage relationships were approximately linear. Examples for cell-attached patches

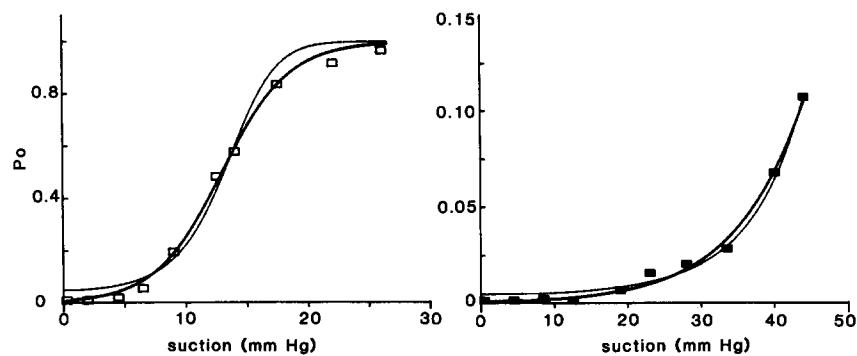


FIGURE 6. Open probability vs. suction relationships for SA (left,  $\square$ ) and RSA (right,  $\blacksquare$ ) stretch-activated channels. Open probability  $P_o$  is plotted vs. negative pressure. The lines are fits to the datapoints with Boltzmann curves (Eq. 1, *thick line* and Eq. 2, *fine line*). Parameters of the fit for the SA channel:  $k = 4.71$ ,  $s = 0.36 \text{ mmHg}^{-1}$  for the linear, and  $k = 2.97$ ,  $s = 1.71 \text{ cmHg}^{-2}$  for the (pressure)<sup>2</sup> model. Parameters for the RSA channel:  $k = 7.25$ ,  $s = 0.12 \text{ mmHg}^{-1}$  for the linear, and  $k = 5.36$ ,  $s = 0.17 \text{ cmHg}^{-2}$  for the (pressure)<sup>2</sup> model. Data from cell-attached patches with one active channel; high  $\text{Na}^+$  solution in the pipette. Holding potentials were at the cell's resting potential (SA) and  $-50 \text{ mV}$  from the cell's resting potential (RSA), respectively.

with  $\text{K}^+$ ,  $\text{Na}^+$ , and  $\text{Ca}^{++}$  as charge carrier through the SA channel are shown in Fig. 7. The slope conductance for  $\text{K}^+$  was found to be highest with  $71 \pm 11 \text{ pS}$  (SD,  $n = 3$ ) followed by  $50 \pm 7.4 \text{ pS}$  ( $n = 5$ ) for  $\text{Na}^+$  and  $23 \text{ pS}$  for  $\text{Ca}^{++}$ . Similar conductances were determined for the RSA channel with  $44 \pm 3.5 \text{ pS}$  ( $n = 6$ ) for  $\text{Na}^+$  and  $22 \pm 3 \text{ pS}$  ( $n = 3$ ) for  $\text{Ca}^{++}$ . Assuming an average resting potential of  $-70 \text{ mV}$ , the extrapolated reversal potentials were  $\sim 0 \text{ mV}$ .

#### *Open- and Closed-Time Distributions*

As mentioned above, SA and RSA channels differ in their gating behavior. Openings of the RSA channel occur in bursts of openings with the time between bursts decreasing with negative pressure (see Figs. 4 and 5). The closed-time distributions showed two components with distinctly different time constants. A fast component

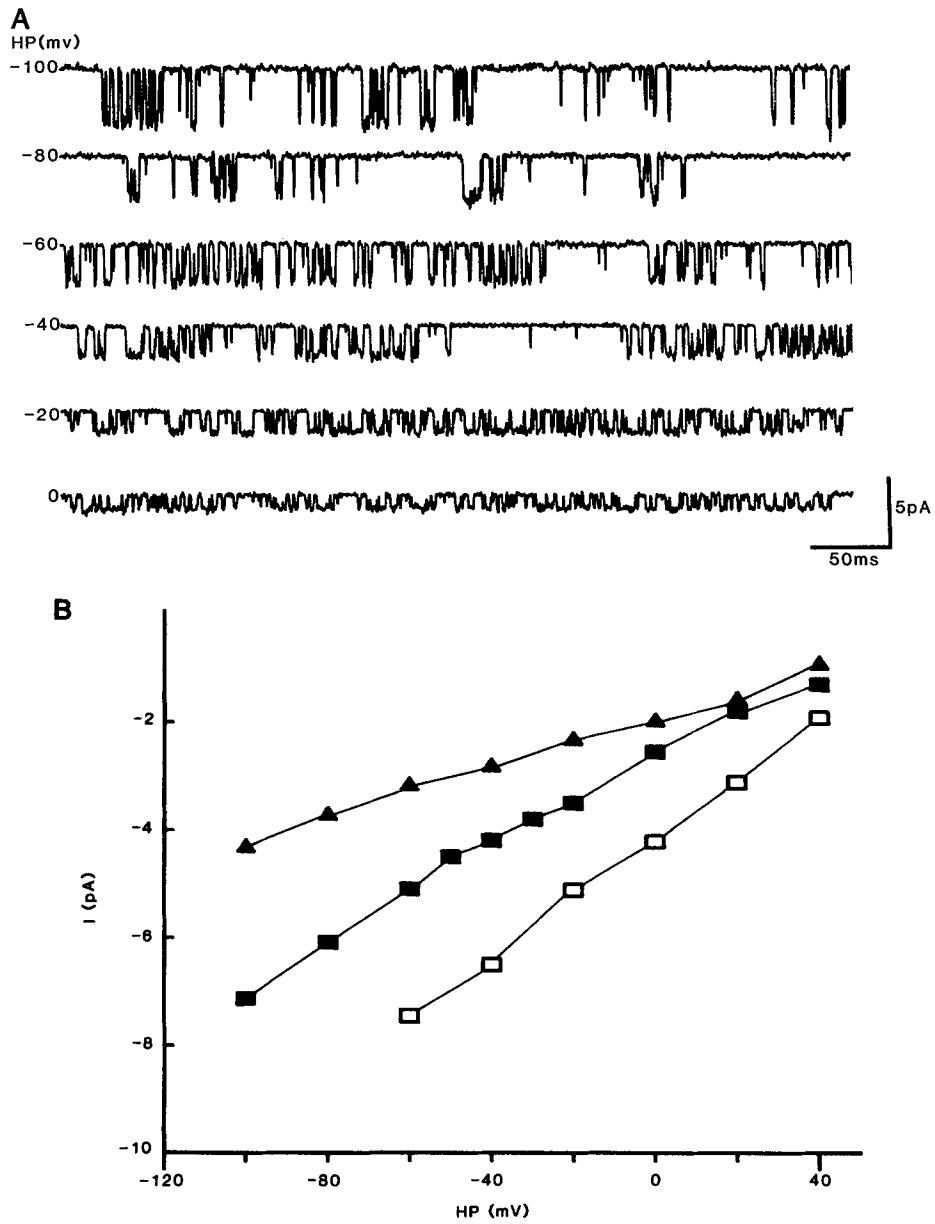


FIGURE 7. Current voltage relationships for unitary currents through SA channels. Cell-attached patches. (A) Single current records at various potentials and 10 mmHg suction. High  $\text{Na}^+$  solution in the pipette. (B) Current-voltage relationships for high  $\text{K}^+$  ( $\square$ ), high  $\text{Na}^+$  ( $\blacksquare$ ), and high  $\text{Ca}^{++}$  ( $\blacktriangle$ ) solutions in the pipette. Potentials are relative to the cells' resting membrane potentials.



ranged from 0.4 to 1.0 ms with no consistent dependence on pressure and represents the short closures during the bursts. The second component, however, varied strongly with pressure. It represents the long closures between bursts and ranged from several seconds at zero suction to some tens of milliseconds at  $-40$  mmHg. Open-time distributions could be best fitted by a single exponential ranging from 0.5 to 1 ms. Again, as with the short closed time, no consistent dependence on negative pressure could be seen.

Gating behavior of the SA channel was considerably more complex. Here two exponentials were necessary to fit the open times and at least three exponentials were needed to describe the closed-time distributions. An example of dwell-time distributions obtained for the SA channel and a plot at different levels of suction are shown in Fig. 8.

#### *Pharmacology of the Stretch-activated Channel*

Neither pressure dependence of the open probability nor other gating parameters of either type of stretch-activated channel were affected by 4-aminopyridine (three patches, 1 mM) and/or tetraethylammonium (two patches, 5 mM) in the pipette solution.

## DISCUSSION

#### *Comparison with Stretch Receptor Data*

The SA-type of stretch-activated cation channel described in this paper fulfills the criteria for the mechanotransduction channel which has been postulated for crayfish stretch receptor neurons (Edwards, 1983). Besides the obvious sensitivity to membrane stretch it has the low cation selectivity previously established for the receptor current in voltage-clamp experiments (Brown et al., 1978; Edwards et al., 1981). The permeability of the channel for  $\text{Ca}^{++}$  is of particular interest in view of the involvement of a Ca-activated  $\text{K}^+$  current in the dynamic phase of the adaptation process (Ottoson and Swerup, 1985*a, b*). The high external  $\text{Ca}^{++}$  concentration in the physiological saline (13.5 mM) is likely to lead to  $\text{Ca}^{++}$  influx through the SA channel and to subsequent activation of  $\text{Ca}^{++}$ -sensitive  $\text{K}^+$  channels. Adaptation at the single-channel level in the sense that the opening probability decreases during sustained membrane deformation, can be excluded from the data presented here.

It is tempting to speculate that the density of stretch-activated channels matches that of the stretch-induced current measured under voltage clamp (Brown et al., 1978). The current data, however, do not allow such a comparison because the patches were from the soma of the receptor cell or, at best, from the primary dendrites. The density of stretch-activated channels is likely to be higher at the dendritic endings, the part of the cell that is actually deformed during stretch of the receptor neuron.

The contribution of the RSA channel to the generator current is unclear, but it is expected to be small since the channel is only active at rather negative potentials (see Fig. 3). Furthermore, the channel density is low compared with that of the SA channel.

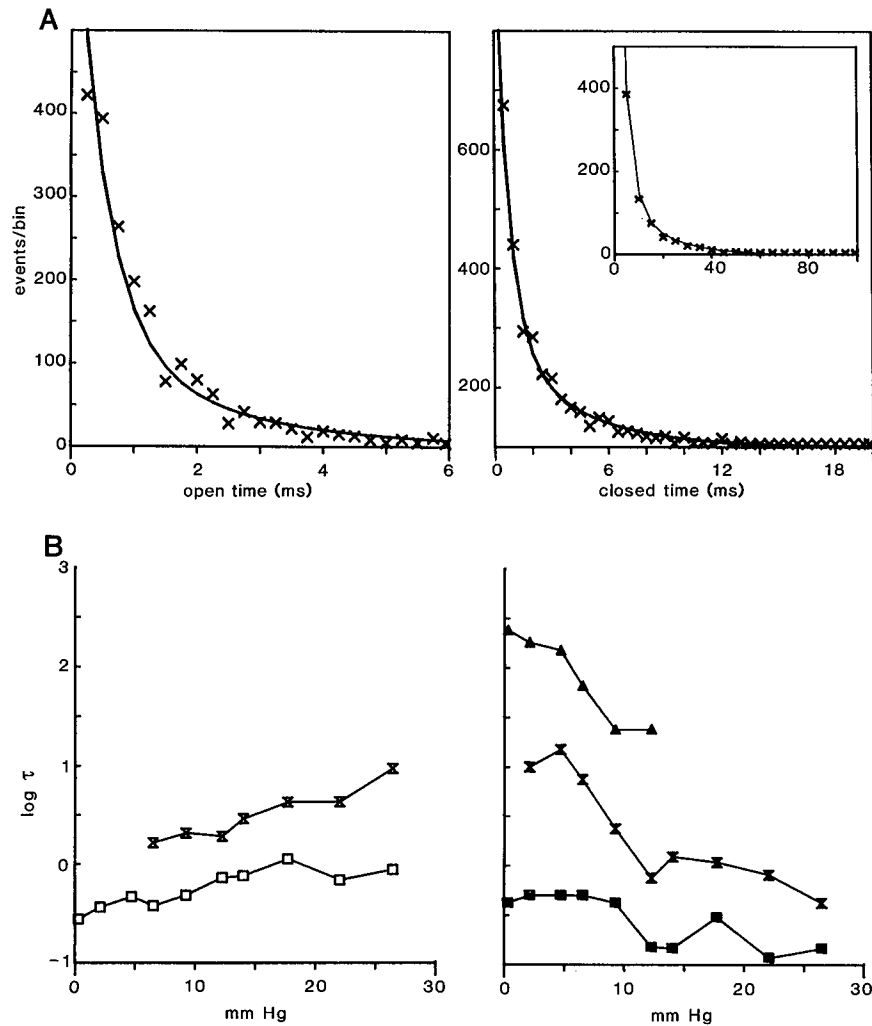


FIGURE 8. Dwell-time distributions for the SA channel. (A) Examples of open- and closed-time distributions at 9 mmHg of suction. Open times were fitted by a double exponential function with time constants of 0.48 and 2.06 ms (0.25 ms bins) and closed times were fitted by the sum of three exponentials with time constants of 0.73, 3.23, and 16.5 ms (0.5 ms bins with the inset replotted with 5 ms bins). (B) Relationships between suction and the logarithm of the dwell times. The two open times are plotted on the left, and the three closed times are on the right.

### Channel Gating

Two models have been proposed to account for the gating of mechanotransduction channels. One is based on the kinetics of the receptor current of hair cells (Corey and Hudspeth, 1983; Holton and Hudspeth, 1986) and the second is based on data from single stretch-activated channels in cultured chick skeletal muscle (Guharay

and Sachs, 1984). While the former model views the stretch-activated channel as a displacement sensor with the gating energy depending on the first order of displacement, the latter assumes the gating energy to be a function of the membrane tension (for the most recent discussion of both models see Howard et al., 1988 and Sachs, 1988). As a consequence, the models predict a linear relationship between either pressure (Howard et al., 1988) or (pressure)<sup>2</sup> (Guharay and Sachs, 1984; Sachs, 1986, 1988) and the natural logarithm of the open probability.

The data on the stretch-activated channels in the stretch receptor neuron presented here were fit by both models (Eq. 1 or 2). The linear model gave a better fit in 3 out of the 10 experiments, the squared model in 1 and no significant difference was found in 6 cases. The difficulty in clearly distinguishing between the two models may result from nonstationary behavior of the channels that produces sufficient scatter. Perhaps for the same reason, the issue of a linear or squared dependence on pressure is controversial in the literature. A linear relationship between the logarithm of  $P_o$  and pressure has been found for a stretch-activated channel in spheroblasts of the bacterium *Escherichia coli* where the channel is possibly involved in volume and osmoregulation (Martinac et al., 1987). Data from a cation selective stretch-activated channel in frog lens epithelium, however, are better fitted by a squared dependence (Cooper et al., 1986).

The average sensitivity of 8.7 mmHg for an  $e$ -fold change in  $P_o$  (linear model) of the RSA channel found in this study is close to the 8 mmHg value found by Martinac et al. (1987) in *E. coli* and, in terms of the squared model (RSA: 0.195 cmHg<sup>-2</sup>; SA: 0.71 cmHg<sup>-2</sup>), similar to the estimates of Guharay and Sachs (1985) (0.66 cmHg<sup>-2</sup>) and those of Cooper et al. (1986) (0.51 cmHg<sup>-2</sup>).

The analysis of dwell times of the RSA channel suggests that only one rate constant, the one that represents the closed times between bursts, is affected by negative pressure. This agrees with data from other stretch-activated channels (Guharay and Sachs, 1984; Sigurdson et al., 1987; Lansman et al., 1987) and also from the transduction channel of hair cells (Holton and Hudspeth, 1986), as inferred from noise analysis.

The use of a 3-kHz bandwidth will bias the measured open and closed times towards longer values, and it is evident from the records that both types of channels show unresolved transitions. Nevertheless, two of the three closed times of the SA channel show significant dependence on pressure (see Fig. 8). A more rigorous study, which is beyond the scope of this paper, will be required to establish a kinetic scheme like that for the stretch-activated channel in embryonic chick skeletal muscle (Guharay and Sachs, 1984). However, the data suggest a more complex kinetic scheme for the stretch-activated SA channel in the crayfish stretch receptor than those for other stretch-activated channels.

I wish to thank Drs. A. Wenning and E. Florey for their comments on the manuscript and Ms. M. A. Cahill for editorial assistance.

This work was supported by the Deutsche Forschungsgemeinschaft (SFB 156/B1).

*Original version received 7 September 1988 and accepted version received 15 May 1989.*

## REFERENCES

- Alexandrowicz, J. S. 1951. Muscle receptor organs in the abdomen of *Homarus vulgaris* and *Palinurus vulgaris*. *Quarterly Journal of Microscopical Science*. 92:163–200.
- Brehm, P., R. Kullberg, and F. Moody-Corbett. 1984. Properties of non-junctional acetylcholine receptor channels on innervated muscle of *Xenopus laevis*. *Journal of Physiology*. 350:631–648.
- Brown, H. M., D. Ottoson, and B. Rydqvist. 1978. Crayfish stretch receptor: an investigation with voltage-clamp and ion-sensitive electrodes. *Journal of Physiology*. 284:155–179.
- Cooper, K. E., J. M. Tang, J. L. Rae, and R. S. Eisenberg. 1986. A cation channel in frog lens epithelia responsive to pressure and calcium. *Journal of Membrane Biology*. 93:259–269.
- Corey, D. P., and A. J. Hudspeth. 1983. Kinetics of the receptor current in bullfrog saccular hair cells. *Journal of Neuroscience*. 3:962–976.
- Edwards, C. 1983. The ionic mechanisms underlying the receptor potential in mechanoreceptors. In *The Physiology of Excitable Cells*. A. D. Grinnell and W. J. Moody, Jr., editors. Alan R. Liss, Inc., New York. 497–503.
- Edwards, C., D. Ottoson, B. Rydqvist, and C. Swerup. 1981. The permeability of the transducer membrane of the crayfish stretch receptor to calcium and to other divalent cations. *Neuroscience*. 6:1455–1460.
- Erxleben, C., and E. Florey. 1988. Stretch-activated single ion channels in the crayfish stretch receptor neurone. *Pflügers Archiv*. 411:R155. (Abstr.)
- Fischer, W., H. Fischer, I. Uerlings, and H. David. 1975. Licht- und elektronenmikroskopische Untersuchungen an den langsam adaptierenden abdominalen Dehnungsrezeptoren des amerikanischen Flußkrebsses *Orconectes limosus* (RAF). *Zeitschrift für Mikroskopisch-Anatomische Forschung*. 89:340–366.
- Guharay, F., and F. Sachs. 1984. Stretch-activated single ion channel currents in tissue-cultured embryonic chick skeletal muscle. *Journal of Physiology*. 352:685–701.
- Guharay, F., and F. Sachs. 1985. Mechanotransducer ion channels in chick skeletal muscle: the effects of extracellular pH. *Journal of Physiology*. 363:119–134.
- Hamill, O. P., A. Marty, E. Neher, B. Sakmann, and F. Sigworth. 1981. Improved patch-clamp techniques for high-resolution current recordings from cells and cell-free patches. *Pflügers Archiv*. 391:85–100.
- Holton, T., and A. J. Hudspeth. 1986. The transduction channel of hair cells from the bull-frog characterized by noise analysis. *Journal of Physiology*. 375:195–227.
- Howard, J., W. M. Roberts, and A. J. Hudspeth. 1988. Mechano-electrical transduction by hair cells. *Annual Review of Biophysics and Biophysical Chemistry*. 17:99–124.
- Lansman, J. B., T. J. Hallam, and T. J. Rink. 1987. Single stretch-activated ion channels in vascular endothelial cells as mechanotransducers? *Nature*. 325:811–813.
- Martinac, B., M. Buechner, A. H. Delcour, J. Adler, and C. Kung. 1987. Pressure-sensitive ion channel in *Escherichia coli*. *Proceedings of the National Academy of Sciences*. 84:2297–2301.
- Methfessel, C., V. Witzemann, T. Takahashi, M. Mishina, S. Numa, and B. Sakmann. 1986. Patch clamp measurements on *Xenopus laevis* oocytes: currents through endogenous channels and implanted acetylcholine receptor and sodium channels. *Pflügers Archiv*. 407:577–588.
- Nadol, J. B., and A. J. D. De Lorenzo. 1973. Observations on the organization of the dendritic processes and receptor terminations in the abdominal muscle receptor organ of *Homarus*. *Journal of Comparative Neurology*. 137:19–58.
- Ottoson, D., and C. Swerup. 1985a. Ionic dependence of early adaptation in the crustacean stretch receptor. *Brain Research*. 336:1–8.
- Ottoson, D., and C. Swerup. 1985b. Effects of intracellular TEA injection on early adaptation of crustacean stretch receptor. *Brain Research*. 336:9–17.

- Sachs, F. 1986. Biophysics of mechanoreception. *Membrane Biochemistry*. 6:173-195.
- Sachs, F. 1988. Mechanical transduction in biological systems. *CRC Critical Reviews in Biomedical Engineering*. 16:141-169.
- Sigurdson, W. J., C. E. Morris, B. L. Brezden, and D. R. Gardner. 1987. Stretch activation of a K<sup>+</sup> channel in molluscan heart cells. *Journal of Experimental Biology*. 127:191-209.
- Tao-Cheng, J.-H., K. Hirosawa, and Y. Nakajima. 1981. Ultrastructure of the crayfish stretch receptor in relation to its function. *Journal of Comparative Neurology*. 200:1-21.
- Woodbury, J. W., and W. E. Crill. 1961. On the problem of impulse conduction in the atrium. In *Nervous Inhibition*. E. Florey, editor. Plenum Publishing Co., New York. 124-135.